



PROPERTIES AND MICROSTRUCTURE OF BRASS UNDER VARIABLE LOADING

S. Mroziński¹, S. Dymski²

¹ University of Technology and Life Science
Department of Machine Design, Mechanical Engineering Faculty
ul. Prof. S. Kaliskiego 7, 85-789 Bydgoszcz, Poland
e-mail: stmpkm@utp.edu.pl

² University of Technology and Life Science
Department of Materials Science and Engineering, Mechanical Engineering Faculty
ul. Prof. S. Kaliskiego 7, 85-789 Bydgoszcz, Poland
e-mail: dysta@utp.edu.pl

Abstract

In the paper there were presented changes of properties and microstructure in the specimens made of CuZn37 brass under fatigue test. During the analysis there were used parameters of hysteresis loop and microstructure changes for different levels of fatigue damage, that were registered during the tests. Basing on the analysis of three hysteresis loop parameters: stress amplitude σ_a , plastic strain amplitude ε_{ap} and plastic strain energy ΔW_{pl} , it has been found that the smallest changes are observed for the energy ΔW_{pl} . Microstructure observations of brass specimens for various damage levels showed that fatigue damage cumulation is also visible in the grains of α phase. Plastic strain of the brass was characterized by the presence of creep strands inside the grains.

Keywords: damage, cyclic properties, failure, creep, brass

1. Introduction

Variable loadings generate in the material of the construction units specific changes and fatigue phenomena. If these loadings are high enough they may locally cause the plastic strains (for example in the notch areas). During fatigue life calculations of the construction units containing areas of the plastic – elastic strains there are used material data defined in the low-cycle fatigue tests [1]. Experimental conditions in this fatigue area are defined i.e. in the standards [2,3]. The characteristic feature of the low-cycle fatigue area is forming, in every cycle of variable loading, of hysteresis loop (Fig. 1).

Characteristic loop parameters i.e. are: total strain amplitude ε_{ac} , plastic strain amplitude ε_{ap} , stress amplitude σ_a and ranges of the mentioned parameters, that is: $\Delta\varepsilon_{ac}$, $\Delta\varepsilon_{ap}$, $\Delta\sigma_a$. The area enclosed by the loop is the measure of the energy dissipated in the material during one loading cycle. This energy is also called the plastic strain energy ΔW_{pl} . Analysis of the mentioned parameters in the function of the loading cycles number enables the description of changes of the cyclic properties of the material and also the course of the damage cumulation. Cyclic strains in

metals and their alloys result in the processes of hardening or softening of the material. They are undoubtedly extraordinary phenomena among many processes that accompany the low-cycle fatigue of metals. At the present moment there is a number of hardening or softening hypotheses. Some of these hypotheses are in connection with hypotheses elaborated for the static loading or they directly result from them. Changes of cyclic properties observed during low-cycle tests are the consequence of the various phenomena and processes which occur in the microstructure of the metals. Description of these processes is possible on the base of analysis of microscopic tests results with the use of dislocation theory.

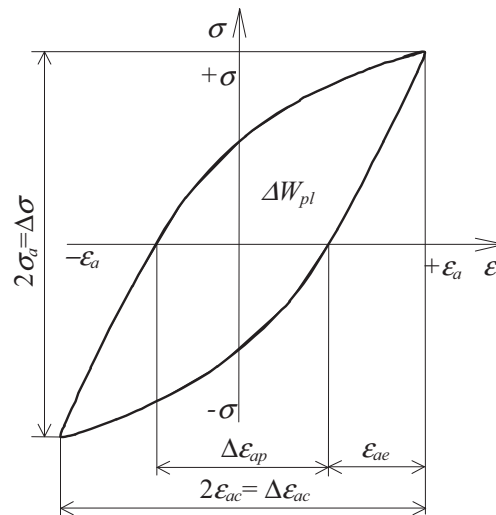


Fig. 1. Characteristic of hysteresis loop parameters

The aim of the paper was analysis of the course changes of the basic hysteresis loop parameters under cyclic loading of one phase alloy - brass with considering metallographic tests.

2. Description of the tests

Fatigue tests were carried out under constant amplitude loadings. They were preceded by the static tests aimed at defining the levels of variable loading. Fatigue tests were performed on six levels of controlled total strain $\epsilon_{ac(1)}=0.35\%$, $\epsilon_{ac(2)}=0.5\%$, $\epsilon_{ac(3)}=0.65\%$, $\epsilon_{ac(4)}=0.8\%$, $\epsilon_{ac(5)}=1.0\%$, $\epsilon_{ac(6)}=1.2\%$. Fatigue tests were performed with the use of the Instron 8501 strength machine. Loading frequency applied in the tests was 0.2 Hz. During the tests momentary values of the loading force and strain of a specimen for chosen loading cycles were registered. Tests parameters were accepted according to directions in the standard [1]. Specimen accepted in the fatigue tests were made of CuZn37 brass. There were two kinds of these specimens: smooth (without a notch) and notched ones. The shape of specimen used in the tests is presented in Fig.2

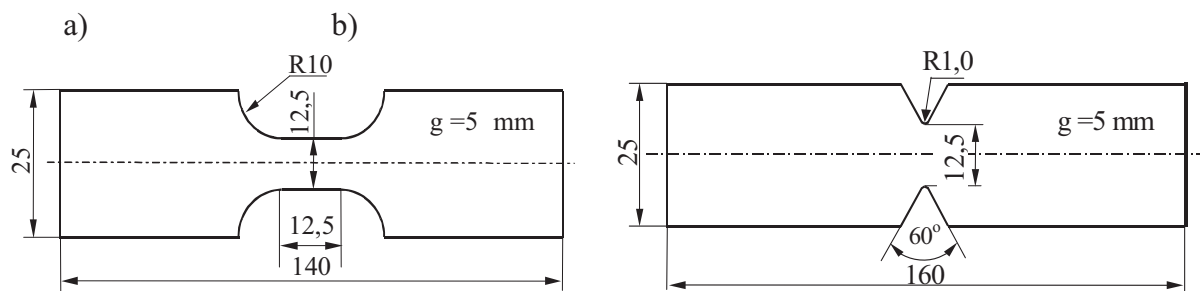
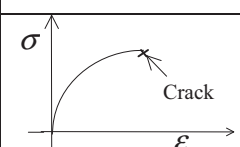
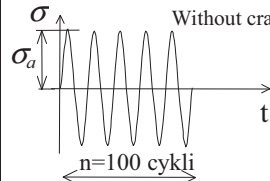
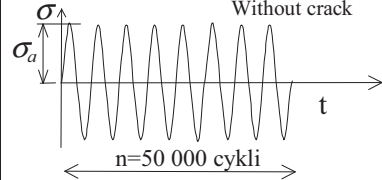
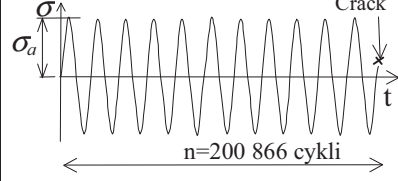


Fig. 2. Specimen used in fatigue tests: a) smooth, b) with a notch

Observations concerning the surface microstructure of specimens were made during the fatigue tests. During microstructure analysis of the fatigue cracks, prof. Kocańda's experiences were widely used [6]. Observations were made for various degrees of fatigue damage. Fatigue damage was defined with the use of so called relative life n/N , where n is the current number of loading cycles and N is the number of cycles until fatigue failure. After realization of the defined number of n cycles for a given loading level the test was stopped and specimens underwent a microscopic examination. Specimens were given this examination in the following situations:

- 1) after static tensile test,
 - 2) after 100 cycles of variable loading ($\sigma_a = 86.4$ MPa), $n/N = 0.002$,
 - 3) after 50 000 cycles of variable loading ($\sigma_a = 86.4$ MPa), $n/N = 0.25$,
 - 4) after 200 866 cycles of variable loading ($\sigma_a = 86.4$ MPa), $n/N = 1$ - failure of the specimen.
- In Tab. 1 there were shown loading diagrams of specimens 1-4 and the ranges of observations.

Tab. 1. Loading diagrams and range of the microscopic observations

Specimen	Scheme of loading	Description of observations
1		Crack and surface of a specimen
2		Surface of a specimen
3		Surface of a specimen
4		Crack and surface of a specimen

Specimens destined for microscopic examinations were specially treated. Their side surfaces in the notch zone were grinded and then polished. After static and fatigue tests there were performed observations of specimen surfaces with the use of light metallographic microscope and scanning electron microscope (SEM). On the specimens there were also taken hardness measurements. Hardness tests were performed with use of the Vickers method under loading of 0.49 N. At each measuring point there were made minimum 5 measurements of hardness. The points of measurement on the specimen were shown in Fig. 3.

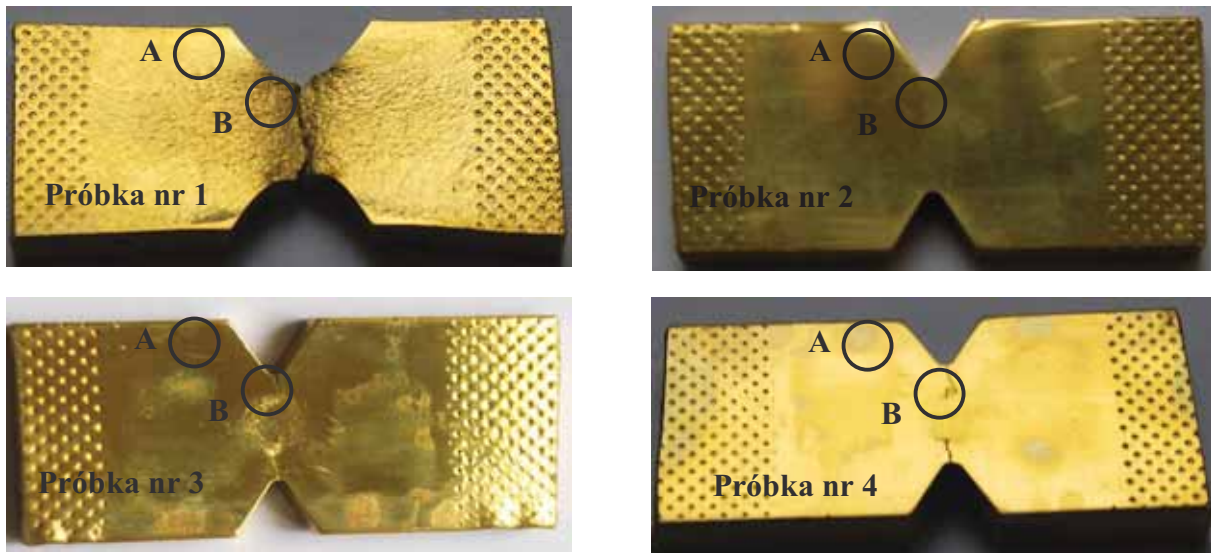


Fig. 3. Points of hardness measurements on the specimens. A – strained zone, B – not strained zone

3. Test results

3.1. Static tests

Static test results were presented in the form of static tensile diagrams of the relation stress σ - relative strain ε . Stress σ values were determined by dividing the momentary loading value of the specimen during the test by its initial cross-section area. An example of the full tensile diagram was shown in Fig. 4a. In Fig. 4b there was shown an initial fragment of this diagram limited to the strains $\varepsilon < 2\%$. In Fig 4b there were also drawn strain amplitude levels accepted during fatigue tests of the specimens.

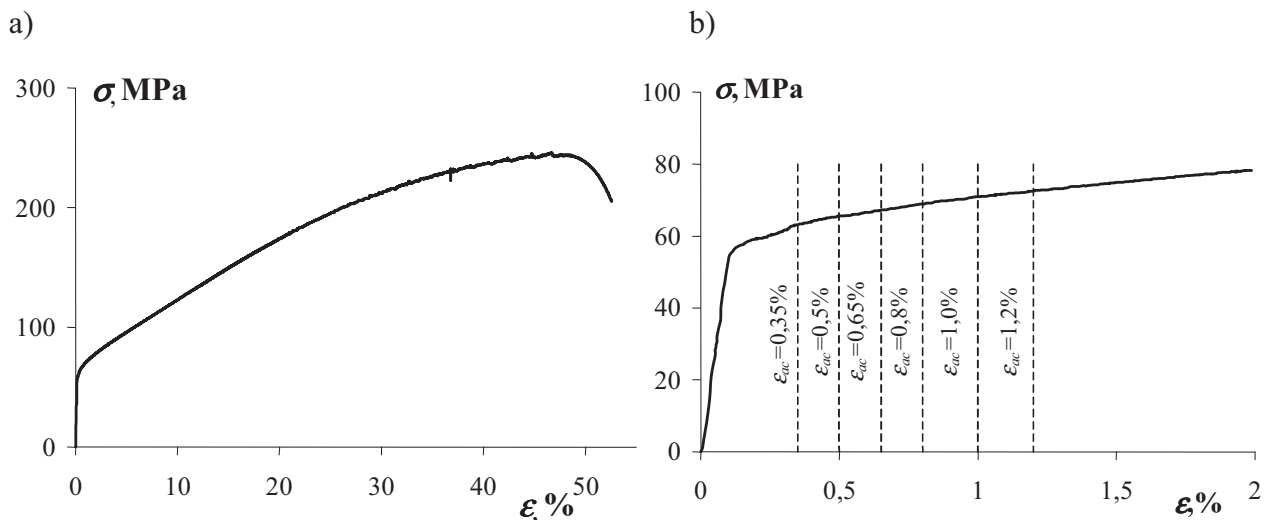


Fig. 4. Static tensile diagrams: a) full diagram, b) initial fragment of the diagram (for $\varepsilon < 2\%$)

3.2. Fatigue tests

During fatigue tests there were observed changes of cyclic properties of tested metal. In order to illustrate the nature of these changes in Fig. 5 there were shown examples of the hysteresis loop

registered during the test at the strain level $\epsilon_{ac}=0.5\%$. Cycles numbers corresponding to the registered hysteresis loops were marked with figures (in the right top of the diagram).

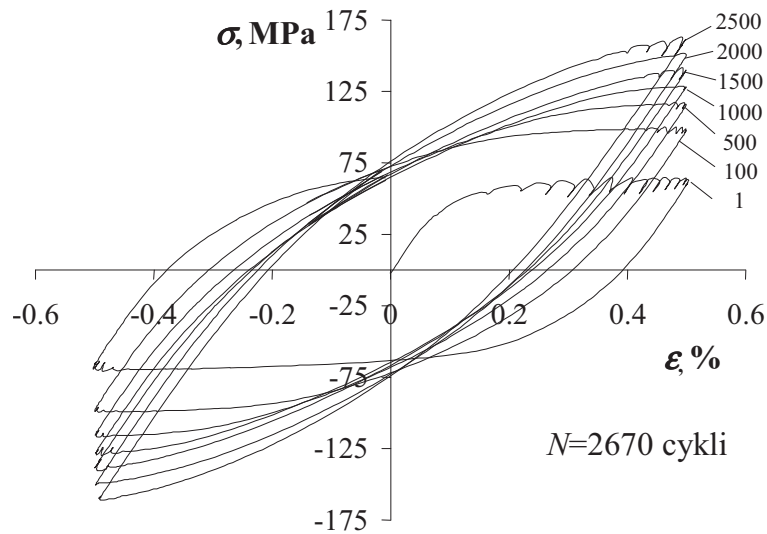


Fig. 5. Hysteresis loops at the strain level $\epsilon_{ac}=0.5\%$

3.3. Microscopic examinations and hardness tests

Surface observations of the 1st specimen in the area of mild plastic strain showed the occurrence of multisystem creeps in grains of α phase. Strain twins were also visible in some grains (Fig. 6a). Specific arrangement of the creep strands in grains determines their boundaries. The arrangement of the creep strands was in agreement with their crystallographic orientation and they had an adequate direction in comparison to the direction of the shear stress action.

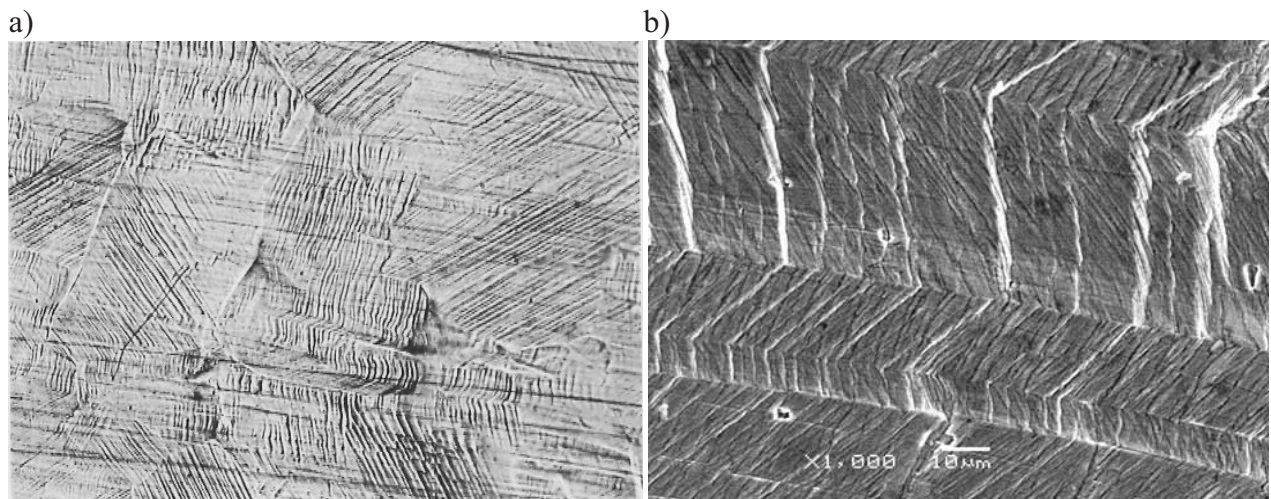


Fig. 6. Microscopic examinations results: a) Multisystem creep in the grains of α phase on the surface of 1-st specimen. 200x magnification, b) Strain twins and permanent creep strands on the surface of the 1st specimen (SEM)

Surface morphology of the 1st specimen next to its crack was shown in Fig. 6b. In grains with very high plastic strain there were found twins and permanent creep strands, i.e. in the form of long filaments – cords [6].

Fatigue failure was initiated on the bottom of the notch near the specimen edge, with significant surface relief. The line of the cracking was orientated at an angle of 90° towards the

loading direction and side surface of specimen. In the initiation zone of the fatigue failure there was observed local plastic strain and it was characterized by the presence of the creep strands in the grains of α phase (Fig. 7a).

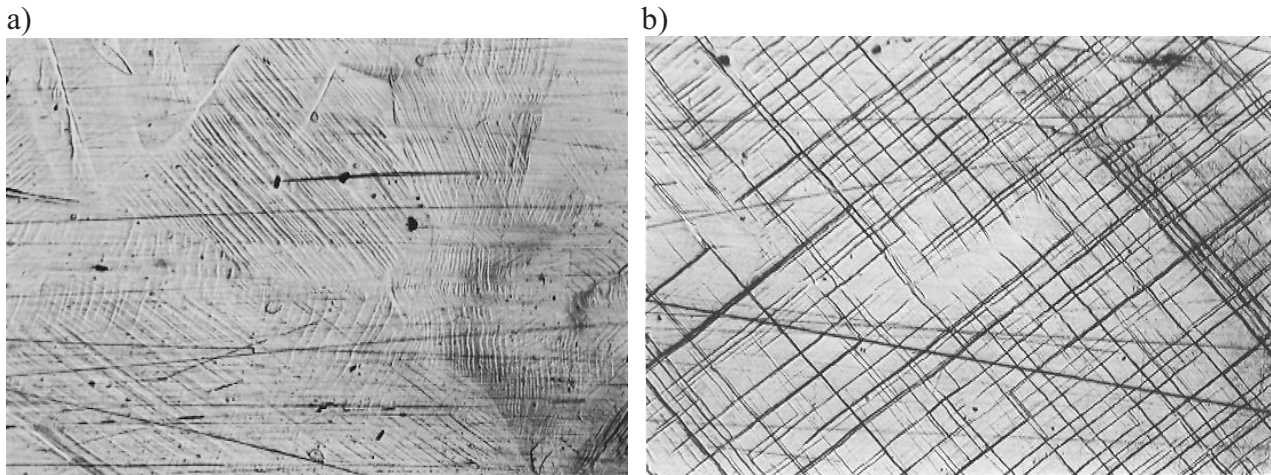


Fig. 7. The strands and creeping lines: a) The creep strands in the grains of α phase on the surface of the 2nd specimen in the initiation zone of failure. 200x magn. ,b) Creeping lines on the surface of the 2nd specimen. 200x magn.

Basing on the microscopic observations along the straight line, connecting notches on the 2nd specimen (Fig. 3), there were found surface irregularities similar to those found on the surface of the 1st specimen in the zone with lower degree of the plastic strain.

On the one of surfaces of the 2nd specimen, near the bottom of the notch, there was found singular set of creeping lines. These lines intersected at an angle of 90° (Fig. 7b). And in relation to the direction of the shear loading, stretch loading and compression loading they were bended down at an angle of about 45° .

On the crack surface of the 4th specimen there were found fatigue stripes that were connected with the creep strands (Fig.8). On the surface of the specimen, just above the edge line and under the second edge of crack, there were visible, beside the creep strands, the extrusions and protusions. However just below the edge of the crack (in the middle of the picture) on its surface there were found the fatigue stripes.

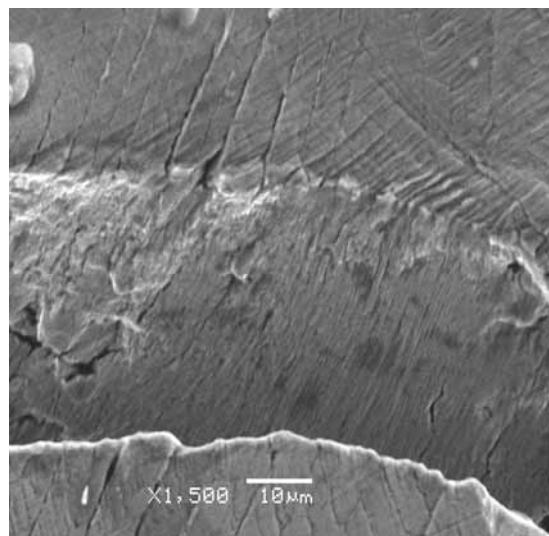


Fig. 8. Microstructure of the fatigue crack and surface of the 4th specimen (SEM)

Hardness measurements results according to the Vickers Method were presented in Tab 2. Measurements were taken in the plastic strain zone – fatigue (A) and in not strained zone (B) (Fig. 3).

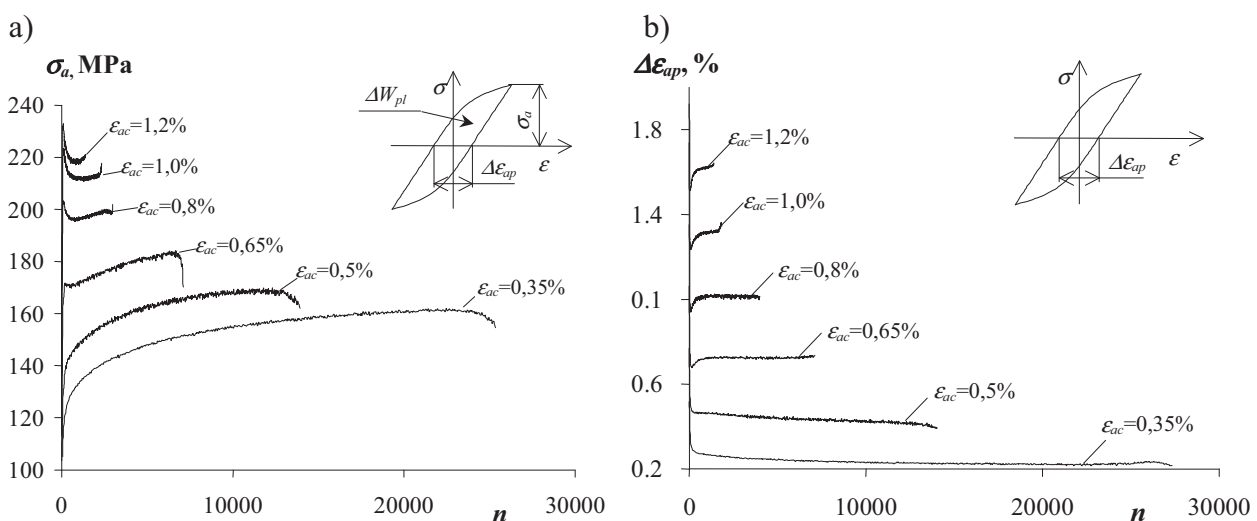
Tab. 2. Hardness of CuZn37 brass on the surface of specimens under static and fatigue tests

Specimen	Measuring point in the zone	Hardness according to Vickers, HV 0.05		
		Measurements	Gap	Arithmetic mean
1	Not strained	119, 117, 122, 119, 122	5	120
	Strained at the edge of the notch	127, 122, 126, 130, 124	8	125
2	Not strained	100, 117, 107, 117,112	17	115
	Fatigue	127, 120, 120, 127, 124, 143, 124, 136, 128, 126 130	23	128
3	Not strained	133, 137, 130, 136, 130	7	133
	Fatigue	101, 101, 101, 112, 101	11	103
4	Not strained	136, 138, 150, 161,146	25	136
	Fatigue	114, 105, 107, 107, 107	7	103

Results of hardness measurements show that specimen 2 hardened in the fatigue zone after $n = 100$ cycles of loading. Its hardness increased by 13 HV 0.05. And in specimens 3 and 4 in the result of variable loading respectively: $n=50\ 000$ and $n=200\ 866$ cycles hardness decreased by 30 and 33 HV 0.05.

4. Analysis of test results

Analysis of hysteresis loops presented in Fig. 5 shows that at the strain level $\epsilon_{ac}=0.5\%$ primary loop parameters such as stress amplitude σ_a , plastic strain range $\Delta\epsilon_{ap}$ and plastic strain energy ΔW_{pl} undergo changes. The shape of the loop and value of its characteristic parameters in the following loading cycles are the proof of brass hardening at this strain level. The momentary values of the loading force and strain registered during the tests at the remaining strain levels were used for calculation of the earlier mentioned hysteresis loop parameters for all strain levels. Their example courses in the function of the loading cycles number were shown in Fig. 9.



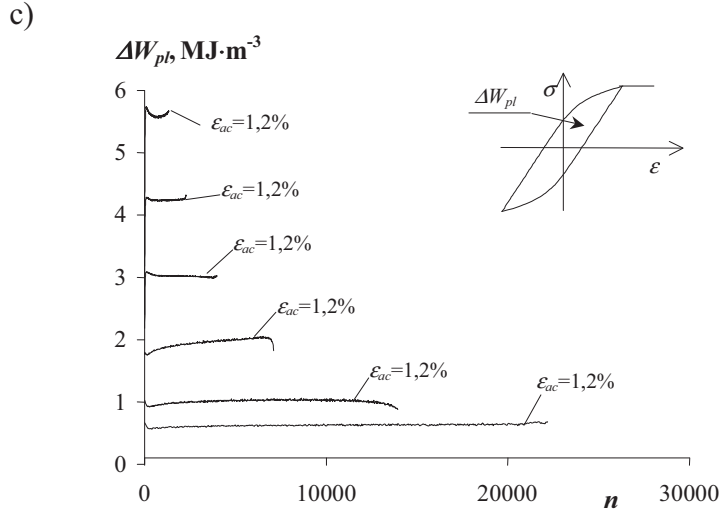


Fig. 9. Changes of hysteresis loop parameters in the function of loading cycles number n for: a) $\sigma_a=f(n)$, b) $\varepsilon_{ap}=f(n)$, c) $\Delta W_{pl}=f(n)$

The course analysis of σ_a , $\Delta\varepsilon_{ap}$ and ΔW_{pl} parameters (Fig. 9) shows that cyclic properties of single-phase brass undergo changes at all levels of strain. For all strain levels cyclic hardening is visible. From the analyzed parameters the least changes in the function of the loading cycles number are observed in the case of the plastic strain energy ΔW_{pl} .

Confirmation of cyclic hardening of brass during variable loading is the mutual position of cyclic and static strain diagrams. Cyclic strain diagram is obtained by approximation of the hysteresis loop apexes at all strain levels with a suitable equation. The most often applied description in the design fatigue analysis is the proposal of the equation given by Ramberg-Osgood [7] in the form :

$$\varepsilon_{ac} = \frac{\sigma_a}{E} + \left(\frac{\sigma_a}{K'} \right)^{\frac{1}{n'}} \quad (1)$$

where:

- E - modulus of elascity, MPa,
- n' - exponent of the cyclic hardening of the material,
- K' - cyclic life coefficient, MPa.

Cyclic strain diagram describing hysteresis loops apexes at all strain levels was presented in Fig. 10.

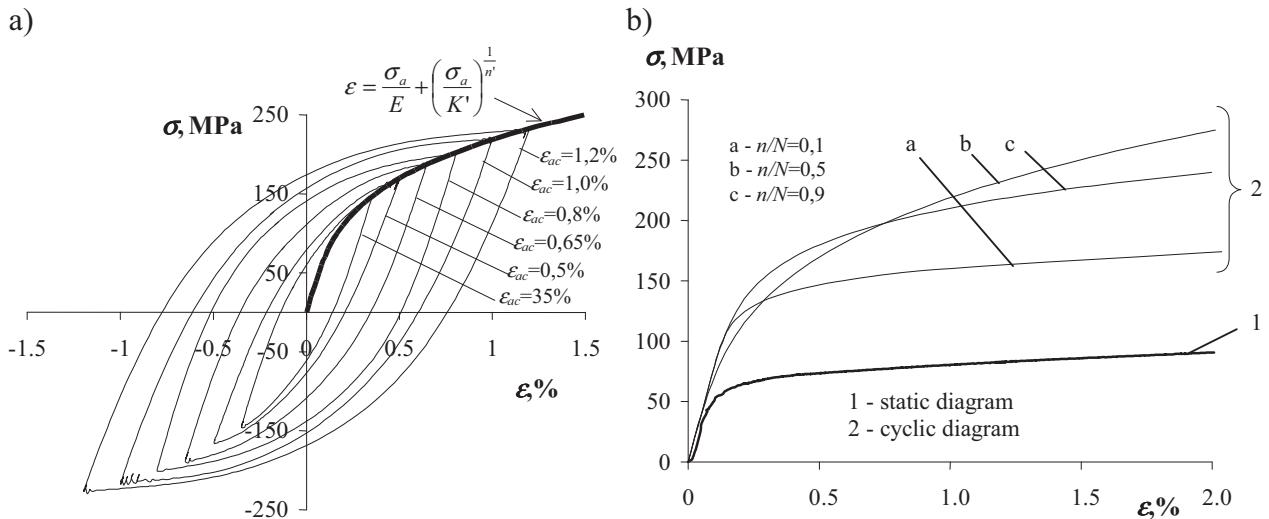


Fig. 10. Investigations results: a) Hysteresis loops from the half-life period ($n/N=0.5$) and cyclic strain diagram, b) Diagrams of static tension (1) and cyclic strain (2)

Hysteresis loops presented in Fig. 12 refer to the damage level corresponding to relative life $n/N = 0.5$. In order to illustrate the scale of changes of cyclic properties of brass during variable loading with the use of the equation (1) in Fig. 13 there were shown diagrams of cyclic strain obtained for the hysteresis loops from various periods of n/N life. There was also shown diagram of the static tension. Position of 2a, b and c curves of the cyclic strain above the diagram of the static tension (1) is the proof of proceeding changes of cyclic properties and the process of metal hardening.

Microscopic tests of specimen surfaces after static and fatigue loading showed microstructure features accompanying fatigue cracking areas. Their characteristic feature is the presence of the creep lines. Detailed analysis of these areas under variable loading enabled the probability valuation of the occurrence and then development of fatigue cracks.

Basing on the microstructure comparative analysis of the specimens under variable and static loading the presence of the similar plastic strain elements was found. Their feature was system of the creep lines originated in the grains of α phase, in agreement with their crystallographic configuration.

Gradual increase of stress during static tensile test resulted in originating, besides the creep systems, the strain twins of α phase (A1 network type). This strain system was also present during fatigue test, but in less degree.

It is given in literature [6] that plastic strain originates in grains with crystallographic orientation in agreement with the direction of easy creep and close to the notches. Therefore a creep in the grains under fatigue test proceeded in the same crystallographic systems as during plastic strain.

Variable loading with participation of plastic – elastic strains brought about the increase of dislocation density in α phase. This in turn resulted in cyclic hardening of the material. As far as crack initiation and development are concern, these processes proceeded under higher loadings.

Brass hardening (Fig. 11) observed in the courses of changes of hysteresis loop parameters was reflected in the results of hardness measurements. On the base of these measurements it was found that in the initial period of life ($n/N < 0.25$) with the increase of loading cycles number hardness of the specimen near the bottom of the notch increased. In this period there also took place the increase of the dislocation density, which in turn resulted in hardening of the material. Further increase of the loading cycles number resulted in insignificant decreasing of specimen hardness in the analysed area in comparison to the initial hardness. It can be the result of the softening of α phase, but only on the surface of specimens. Yet from fatigue tests resulted brass hardening.

Decreasing of the material hardness in the crack area on the stage of its development, demands further investigations based upon the stability of dislocation structure, originating during fatigue failure.

5. Summary

Changeability of the hysteresis loop parameters in the function of the loading cycles number causes that the values of the material data used during fatigue life calculations depend on the life period in which they were determined. In consequence the methods of fatigue life calculations based on the assumption of cyclic properties stabilization during variable loadings raise doubts.

The small changes of the plastic strain energy ΔW_{pl} in the function of loading cycles number observed during the tests are the confirmation of the literature data [3]. It results from them that energy parameter is the least sensitive to the changes of cyclic properties of material. It is motivated by the fact that the energy parameter takes into account mutual interactions of both stress and strain. Because of that fact it is believed that an energy approach to fatigue process is more complete than strain or stress description.

Changes of material properties under variable loading are influenced by dislocation structure. With the increase of fatigue damage degree dislocation density increases too, which results in cyclic hardening.

Presently there exist many models of the course of material hardening mechanism. One of the best known is the Granato-Lücke mechanism [5]. Analysis of this mechanism and obtained tests results allow to conclude that observed cyclic hardening of brass specimens was the result of creating the obstacles for dislocation movement, with their mutual interaction.

Obtained results confirm literature reports that pure metals and one-phase alloys after annealing can undergo cyclic hardening [6]. Hardening of α phase was confirmed by the fatigue tests (Fig. 13).

In the boundary layers of the specimens with the increase of the loading cycles number the creep lines turn into so called permanent creep strands which are different from the creep strands originating during static plastic strain. Permanent creep strands in the grain structure placed themselves on the surface of the specimen. Formation of the permanent creep strands resulted in the change of properties, decreasing of the plasticity limit also included, since inside of them intensive irreversible softening took place [6].

In literature there are also reports stating that plastic strain amplitude in the permanent creep strands is higher than in groundmass. It is the proof of existing diversified dislocation structure in the permanent creep strands and groundmass.

Decreasing of the dislocation density in the permanent creep strands results in the softening of the material under cyclic loading. So the explanation of the softening can refer only to the sub-boundary layer of the specimen, to the depth of only one or several grains. Performed investigations proved that all specimens under fatigue tests underwent the process of hardening in the whole cross-section.

On the base of the performed analysis of obtained results the following conclusions were formulated:

1. The course of the chosen hysteresis loop parameters in the fatigue test depends on the strain level. The values of these loop parameters, in turn, depends on the degree of fatigue damage.
2. Plastic strain energy ΔW_{pl} in the function of the loading cycles number is the least sensitive parameter to the changes of cyclic properties of CuZn37 brass.
3. Microstructure of the surface of the fatigue specimens presented the features of the plastic strain.
4. Acceptance in the tests of one – phase brass contributed to the partial explanation of the phenomena taking place during fatigue tests of the material with the use of light microscope and scanning electron microscope (SEM).

References

- [1] Tucker, L.E., *A Procedure for Designing Against Fatigue Failure of Notched Parts*, Society of Automotive Engineers, Inc., SAE Paper No 720265, New York 1972.
- [2] PN-84/H-04334: *Badania niskocyklowego zmęczenia metali*.
- [3] Kocańda, S., Kocańda, A., *Niskocyklowa wytrzymałość zmęczeniowa metali*, PWN Warszawa 1989.
- [4] Kocańda, S., *Zmęczeniowe pękanie metali*. WNT, Warszawa 1985.
- [5] Kocańda, S., Kocańda, D., *Fraktografia. Badania mikrobudowy przelomów zmęczeniowych w latach 1954-2004*, Przegląd mechaniczny R.LXIV, Z1 (2005).
- [6] Wyrzykowski, J.W., Pleszakow, E., Sieniawski, J., *Odkształcenie i pękanie metali*, WNT, Warszawa 1999.
- [7] Ramberg, W., Osgood, W.R., *Description of stress-strain curves by three parameters*, NACA, Tech.Note, No. 402, 1943.

The paper was elaborated on the base of the research studies BS-4/2002 under the title "Experimental methods in the fatigue tests of the materials and construction elements" which were carried out in the Faculty of Mechanical Engineering in 2009.

